

Structure and Function of Chihuahuan Desert Ecosystem  
The Jornada Basin Long-Term Ecological Research Site  
Edited by: Kris Havstad, Laura F. Huenneke, William H. Schlesinger  
Chapter 15 Rango, A., Ritchie, J., Schmutge, T., Kustas, W., Chopping, M.J. 2006



Submitted to Oxford University Press for publication  
ISBN 13 978-0-19-511776-9

## 15

### Applications of Remotely Sensed Data from the Jornada Basin

**Albert Rango, Jerry Ritchie, Tom Schmutge, William Kustas, and Mark J. Chopping**

Like other rangelands, little application of remote sensing data for measurement and monitoring has taken place within the Jornada Basin. Although remote sensing data in the form of aerial photographs were acquired as far back as 1935 over portions of the Jornada Basin, little reliance was placed on these data. With the launch of Earth resources satellites in 1972, a variety of sensors have been available to collect remote sensing data. These sensors are typically satellite-based but can be used from other platforms including ground-based towers and hand-held apparatus, low-altitude aircraft, and high-altitude aircraft with various resolutions (now as good as 0.61 m) and spectral capabilities. A multispectral, multispatial, and multitemporal remote sensing approach would be ideal for extrapolating ground-based point and plot knowledge to large areas or landscape units viewed from satellite-based platforms. This chapter details development and applications of long-term remotely sensed data sets that are used in concert with other long-term data to provide more comprehensive knowledge for management of rangeland across this basin and as a template for their use for rangeland management in other regions.

In concert with the ongoing Jornada Basin research program of ground measurements, in 1995 we began to collect remotely sensed data from ground, airborne, and satellite platforms to provide spatial and temporal data on the physical and biological state of basin rangeland. Data on distribution and reflectance of vegetation were measured on the ground along preestablished

transects with detailed vegetation surveys (cover, composition, and height); with hand-held and yoke-mounted spectral and thermal radiometers; from aircraft flown at different elevations with spectral and thermal radiometers, infrared thermal radiometers, multispectral video, digital imagers, and laser altimeters; and from space with Landsat Thematic Mapper (TM), IKONOS, QuickBird, Terra/Aqua-MODIS and -ASTER, NOAA-AVHRR, and GOES satellites. These different platforms (ground, aircraft, and satellite) allow evaluation of landscape patterns and states at different scales. One general use of these measurements will be to quantify the hydrologic budget and plant response to changes in components in the water and energy balance at different scales and to evaluate techniques of scaling data.

Our concept involves overlaying various remote sensing capabilities at the same time in an area that has been studied for a long time using conventional approaches and where ground measurements can be taken at the time of the remote sensing observations. Jornada Basin study sites are ideal for this approach. The same types of data are acquired from different platforms with varying detail of measurement and with the objective of developing a way to spatially scale up or down and provide increased information content. Data have covered parts of both the Jornada Experimental Range (JER) and the Chihuahuan Desert Rangeland Research Center (CDRRC).

### **Conventional and Remote-Sensing Ground Measurements**

These data were collected for comparison with aircraft- and satellite-measured radiance and reflectance. Sites (figure 15-1) were established in each of the five major vegetation types: black grama (*Bouteloua eriopoda*) upland grasslands, tobosa (*Plueraphis mutica*)-dominated playas, creosotebush (*Larrea tridentata*) shrublands, mesquite (*Prosopis glandulosa*) dune systems, and

tarbush (*Flourensia cernua*) shrublands (as used for aboveground net primary production estimates as described in chapter 11).

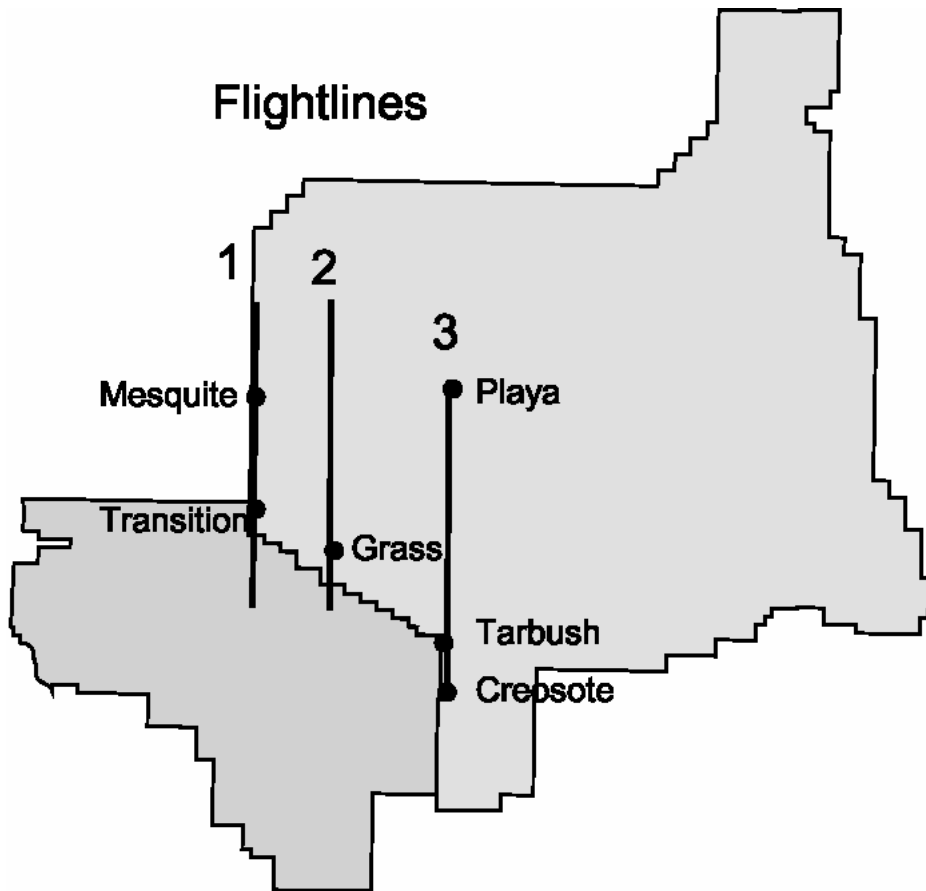


Fig. 15-1. Jornada Experimental Range and Chihuahuan Desert Rangeland Research Center map with locations of six sites and the primary low-altitude aircraft flight lines.

An additional site was located in an area of transition between the black grama grassland and the mesquite dune system. At these six sites both a 150-m permanently marked linear transect and a 30- × 30-m, 49-point square grid with grid points 5 m apart were established with remote sensing overflights in mind. Linear transects were used for vegetation surveys, leaf area index observations, and hand-held, full-range spectroradiometer measurements. Vegetation

measurements were made of species cover, maximum plant height, and standing litter using vertical line-point intercept techniques (Canfield 1941; Eberhart 1978). In general, as ground cover decreased from grass to transition to mesquite communities, reflectance measured from all instruments increased, indicating a potential for change in heat and water balance of these ecosystems if shrubs continue to expand into the grass communities. These data suggest that changes of vegetation from grass-dominated to mesquite-dominated communities in the Jornada Basin could have significant effects on the albedo and the surface temperatures measured at the different sites and on the overall water and energy budget within the basin.

Leaf area index (LAI) measurements were made with a LICOR LAI-2000 instrument. Measured LAI has varied greatly over the time period (table 15-1) and trends are difficult to determine.

In general, LAI is higher at the grass site in the spring (May) than in the fall (September/October). At the transition site the reverse is generally true; namely, the LAI is higher in fall than in spring. The mesquite site LAI has no consistent pattern, whereas the creosote site, over a more limited number of years, generally has a greater LAI in spring. LAI was low at all sites in September 2001. Variability in the range of LAI has increased since 1995 with great fluctuations in measurements in recent years.

Radiometric plant canopy and soil reflectance measurements were made with a Barnes modular multispectral radiometer at the grass, transition, and mesquite sites in September 1995 and September 1996 (Everitt et al. 1997). Spectral radiance measurements were made between 1100 and 1400 hours under sunny conditions. Radiometric measurements were converted to

Table 15-1. Average leaf area index measure along 150-m transects at the Jornada Experimental Range with an LAI-2000.

Date	Grass	Transition	Mesquite	Creosote	Tarbush	Playa
September 1995	0.77	0.93	1.03			
February 1996	0.99	0.80	0.52			
May 1996	0.96	0.68	0.91			
September 1996	1.32	1.58	0.95			
May 1997	0.71	0.69	1.17			
September 1997	0.68	0.70	0.72			
April 1998	0.54	0.41	0.38			
September 1998	0.30	1.15	1.51	nd		
May 1999	0.83	0.22	0.25	2.18		
September 1999	0.83	1.06	1.54	1.69		
May 2000	0.47	0.66	1.66	1.27		
September 2000	0.31	0.97	1.25	0.75		
May 2001	1.36	1.37	1.89	2.13	nd	
September 2001	0.51	0.71	0.37	0.66	1.54	
May 2002	1.27	0.90	1.91	1.89	1.62	
October 2002	0.85	0.35	0.50	0.80	0.82	nd
May 2003	0.68	0.49	1.30	0.93	1.29	1.96

reflectance for a common solar irradiance reference condition (Richardson 1982). Additionally, multispectral measurements were made using an Exotech four-band radiometer, corresponding to the first four bands of Landsat TM and mounted on a shoulder-configured yoke system to measure the 30- × 30-m grid points and along the transect. A thermal radiometer was also mounted on the yoke.

Spectral radiance of vegetation communities were measured at 1 m above ground level using an Analytical Spectral Device (ASD) spectrometer at the 30- × 30-m grids at 5-m intervals

and along the vegetation transects. The ASD makes measurements from 0.350–2.500  $\mu\text{m}$  at 0.001- $\mu\text{m}$  intervals. At each study site, separate radiometric measurements were made for each frequently encountered plant species, litter, and bare soil (10 measurements of each selected cover type). ASD spectral radiance measurements made on the  $30 \times 30 \text{ m}^2$  grids at 5-m intervals for the grass, transition, mesquite, and creosote sites for May and September 2001 were averaged to simulate a  $30\text{-m}^2$  pixel. All sites have similar overall radiance patterns over the entire spectrum (0.350–2.500  $\mu\text{m}$ ).

Though the spectra patterns are similar, there are differences in the magnitudes of radiance measured over the different vegetative communities. Mesquite communities have the highest reflectance with the exposed soil cover fraction up to 0.75. The transition communities have the next highest radiance, followed by the grass communities. The creosote and tarbush communities are usually between the grass and transition communities. Both of these communities have significant grass cover between and under the creosote and tarbush shrubs.

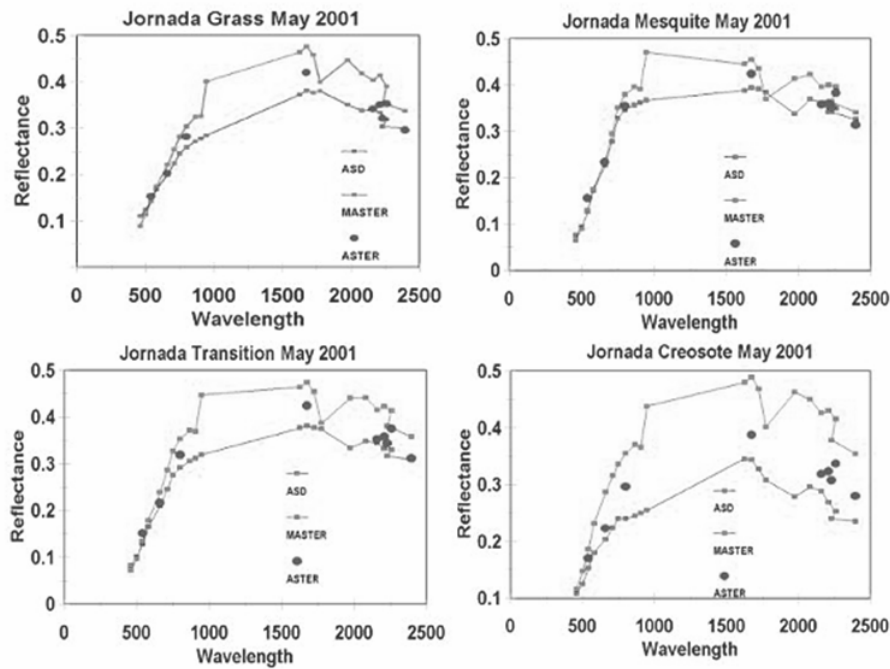


Fig. 15-2. Radiance measurements for May 2001 for different cover types (bare soil, mesquite *Prosopis glandulosa* and grass) at the Jornada Experimental Range. Data are the average of 10 measurements directly over each cover type taken with the Analytical Spectral Device Spectrometer.

MODIS and ASTER are multispectral sensors on Terra, NASA's Earth Observation System (EOS) satellite. MASTER is the MODIS-ASTER simulator and has 50 channels from the visible to the thermal infrared (TIR), again with 2.5 mrad IFOV and a swath of about 45°. A comparison of reflectance measurements from the ASD, MASTER, and ASTER instruments showed that reflectance increased from grass to transition to mesquite communities from all three platforms (Figure 15-2). Patterns of reflectance were similar from the three platforms with MASTER and ASTER having similar absolute values. Comparison of absolute values of ASD ground measurements with MASTER and ASTER measurements differed with different vegetation communities, but in general, ASD reflectance measurements were slightly lower than



MASTER or ASTER measurements. These differences are assumed to be related to the different footprint sizes of the instruments and probably the lesser percent of base soil cover in the ASD footprint.

Ground-based multiangular reflectance measurements have been acquired as part of the NASA EOS Grassland PROVE (prototype validation exercise) (Privette et al. 2000) field campaign and from 1999–2002 as part of our program (Rango et al. 1996; Ritchie et al. 1996). The PROVE data sets were acquired by a team from the University of Nebraska-Lincoln using a short tilting mast to acquire off-nadir samples over the semi-natural grassland, soil, and shrubland surfaces. Our data sets were acquired primarily in support of aircraft multiangle campaigns using a similar apparatus. At times a boom truck with a 30-m-high extension capability was used to measure sky and surface radiance.

From 1995 to 2000, surface landscape (soil and vegetation) temperatures were measured with an Everest thermal infrared radiometer (IRT) with a band pass of approximately 8–13  $\mu\text{m}$ . Since 2000, temperature measurement has been made with an Apogee radiometer recorded on a Fluke thermometer.

Surface energy fluxes have been monitored on a nearly continuous basis from 1995 to 1997 using the Bowen ratio energy balance method (BREB). During the episodic field campaigns from 1997 through 2002 and continuously since May 2002, they have been monitored with eddy correlation (EC) and Bowen ratio systems primarily at grass and mesquite locations.

The Radiation and Energy Balance System (REBS) surface energy balance system (SEBS) was installed primarily at grassland and mesquite dune sites to measure energy flux, weather, and supplementary data. The SEBS is an integrated system of sensors designed for the

U.S. Department of Energy's Atmospheric Radiation Measurement program. The net radiation ( $R_n$ ) was measured using a REBS Q7 net radiometer positioned between 2 and 3 m above the surface. Air temperature and vapor pressure differences were measured with modified Vaisala HMP35A temperature-humidity probes with a 2-m separation.

Wind speed and direction were measured using a Met One anemometer and wind vane located at a nominal height of 3 m above the local topography. Atmospheric pressure was measured using a Met One barometric pressure sensor at one of the sites. Soil moisture was measured at over 5 cm depth using three soil moisture resistance sensors (REBS SMP-2). This value of soil moisture was used with an estimate of bulk density to compute the soil heat capacity, which is then used with a time rate of change in soil temperatures.

EC measurements were made using a one-dimensional Campbell Scientific CA27 with fine-wire thermocouple and, in later years, using a three-dimensional Campbell Scientific CSAT3 sonic anemometer to measure vertical wind speed ( $w$ ) and air temperature ( $T$ ) and a KH20 krypton hygrometer to measure vapor density ( $\rho_v$ ) (Tanner et al. 1985; Tanner 1988).

Preliminary analyses of the BREB and EC data indicate significant discrepancies in flux estimates between the two techniques, particularly for the mesquite dune site where heterogeneity (distances between dune and mesquite clumps) exists at scales of tens of meters (Hippis et al. 1977; Ramalingam 1999). In general,  $H$  estimated by the BREB method tended to be significantly higher than when measured by the EC method; interestingly, the  $\lambda E$ -values were somewhat smaller. This results in the BREB method estimating a larger value of the Bowen ratio  $\beta$  ( $= H/\lambda E$ ) than given by the EC system.

The BREB method assumes that available energy ( $R_n - G$ ) can be measured without

error. For uniform surfaces with large values of vertical gradients, the Bowen ratio technique works well. However, there are serious problems for heterogeneous surfaces because some of the assumptions are simply not valid (Hipps and Kustas 2001). In fact, a recent study by De Bruin et al. (1999) suggests that many environmental and landscape conditions existing in desert environments are likely to cause a breakdown in temperature-humidity similarity and, hence, in the equality of the eddy diffusivities. However, differences in flux estimates between EC and BREB methods over heterogeneous terrain are usual. For example, similar discrepancies were observed over more uniform grasslands (Fritschen et al. 1992).

Efforts continue to evaluate and understand the factors causing discrepancies between the turbulent heat fluxes estimated by BREB and EC methods, but there have also been detailed studies of the uncertainty in measuring  $R_n$  and  $G$  for these desert communities. Not only is the available energy a necessary quantity for computing the heat fluxes using the BREB method, it is also a common approach for gaining a level of confidence in the turbulence flux measurements by assessing the closure ratio (CR) defined as  $(H + \lambda E)/(R_n - G)$ . The value of CR is generally less than 1 and may be due to a number of factors, including sensor measurement errors, horizontal flux divergence, and a significant mismatch in source areas of the measured fluxes (Stannard et al. 1994). For these sparsely vegetated surfaces, the mismatch in source areas is likely to be extreme between the measurement of available energy and the heat fluxes.

For net radiation, Kustas et al. (1998) showed that different models of radiometers from the same manufacturer required recalibration to achieve an uncertainty of less than 5% for this particular environment. Net radiometers from different manufacturers could also be made to agree under a dry condition by using regression or autoregression techniques. However, the

resulting equations would induce bias for the wet surface condition. Thus, it is not possible to cross-calibrate two different makes of radiometers over the range of environmental conditions observed. This result indicates that determination of spatial distribution of net radiation over a variable surface should be made with identical instruments that have been cross-calibrated. However, the need still exists for development of a radiometer and calibration procedure that will produce accurate and consistent measurements over a range of surface conditions (Kustas et al. 1998).

Kustas et al. (2000) used an array of 20 soil heat flux plates and soil temperature sensors to characterize the spatial and temporal variability in soil heat flux as affected by vegetation and microtopographic effects of mesquite dune communities. Maximum differences in soil heat flux among sensors were nearly  $300 \text{ W/m}^2$ . Maximum differences among individual sensors under similar cover conditions (i.e., no cover or interdune, partial or open canopy cover, and full canopy cover) were significant, reaching values of  $200\text{--}250 \text{ W/m}^2$ . The “area average” soil heat flux from the array was compared to an estimate using three sensors from the nearby BREB station. These sensors were positioned to obtain soil heat flux estimates representative of the three main cover conditions, namely, no cover or interdune, partial or open canopy cover, and full canopy cover. Comparisons between the “array average” soil heat flux and the three-sensor system indicate that maximum differences on the order of 50 to nearly  $100 \text{ W/m}^2$  are obtained in the early morning and midafternoon periods, respectively. These discrepancies are caused by shading from the vegetation and microtopography. The array-derived soil heat flux also produced a significantly higher temporal-varying, soil heat flux/net radiation ratio than that observed in other studies under more uniform cover conditions. Results from this study suggest

that microtopography, as well as clustering of vegetation, needs to be accounted for when determining the number and location of sensors needed for estimating area average soil heat flux in this type of landscape.

Future investigations will include source-area footprint analyses (e.g., Schuepp et al. 1990; Schmid and Oke 1990; Horst and Weil 1992) to assess surface properties of the upwind fetch affecting the measurements. High-resolution remote sensing data will be critical for evaluating the surface properties within each of the source-area footprints. In addition, the 20-Hz turbulence data collected from recent experiments in 2000 and 2002 will be used to explore the applicability of the Monin-Obukhov similarity theory (MOST), relating mean and variance to covariance statistics (i.e., flux-gradient and flux-variance similarity) of temperature, humidity and momentum (wind) for the different desert communities. This work will ultimately prove useful for assessing the utility of MOST because land-atmosphere transfer schemes used in atmospheric models and remote-sensing energy balance approaches rely on MOST parameterizations (Hipps and Kustas 2001).

### **Low-Altitude Aircraft Missions**

Laser profile altimetry measurements were made on four north-south and four east-west flight lines designed to cross the three study sites. Laser altimetry flights were made in May 1995, September 1995, February 1996, and May 1997. Flights were made at an altitude of approximately 200 m AGL. The altimeter was a pulsed gallium-arsenide diode laser transmitting and receiving 4,000 pulses per second at a wavelength of 0.904  $\mu\text{m}$ . The field of view of the laser was 0.6 milliradians, which gives a footprint on the ground that is approximately 0.06% of the altitude. The timing electronics of the laser received allowed a vertical resolution of 5 cm for

each measurement.

Laser altimeter-measured transects at the black grama grass, mesquite, and transition sites show differences in surface topography and roughness at the sites. The grass site (figure 15-3) is relatively uniform in surface roughness with an occasional shrub or taller vegetation on the surface present on the underlying topography.

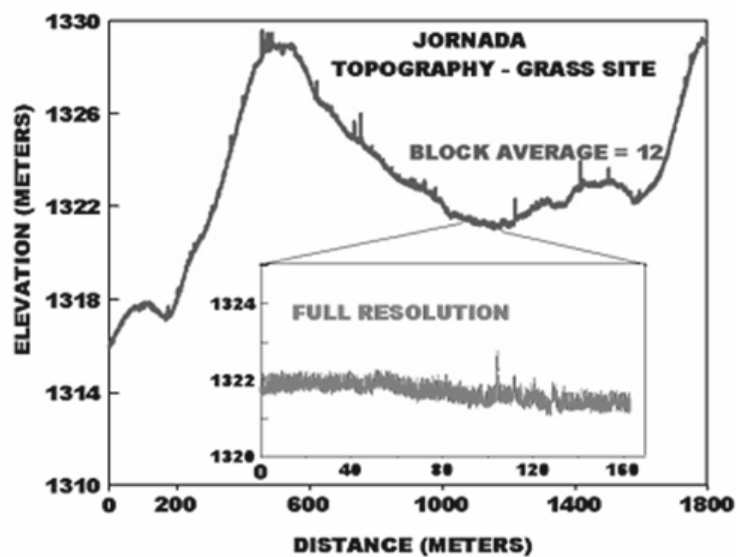


Fig. 15-3. Laser altimeter measurement of topography and surface roughness at the grass site on May 19, 1995 at the Jornada Experimental Range.

The mesquite site has evidence of dunes present on the underlying landscape with vegetation on top of the dunes. The transition site shows similarities to both the grass and mesquite sites with the beginning of what appear to be small dunes. Fractional vegetation cover and vegetation height measured from the laser altimeter data were comparable to measurements made on the ground (Ritchie 1996).

Fractal analysis of laser altimetry data from the grass, mesquite, and transition sites (four

transects at each site for February, May, and September) supports the possibility of distinguishing between these landscapes using fractal properties of the laser data. A specific range of scales of fractal dimension can be used for distinguishing between grass, mesquite, and transition landscapes. The fractal dimensions tend to increase in a sequence from grass to transitional to mesquite sites in this range of scales. A fractal technique for estimating cover type represents a new technical opportunity to quantify landscape roughness (Pachepsky et al. 1997; Pachepsky and Ritchie 1998).

Studies have also shown (Menenti and Ritchie 1994; Menenti et al. 1996) that the effective aerodynamic roughness at the shrub site can be estimated using the high-resolution laser altimeter measurements of land surface roughness. Studies at the mesquite site on the Jornada show that estimations of aerodynamic roughness and displacement height of a complex terrain, consisting of coppice dunes with bare interdunal areas, are plausible using simple terrain features computed from high-resolution laser altimeter data (De Vries et al. 1997, 2003).

A scanning laser altimeter was flown over the sites in February 1998. The laser instrument was the Swedish Saab/TopEye system flown on a helicopter platform using an across-track scanning system with a Z-shaped ground target path and with the along-track sampling rate determined by the speed of the aircraft. The wavelength of the laser is in the near infrared at 1.064  $\mu\text{m}$ . The instrument operates in a number of modes, providing a sampling density adjustable from 1–15 samples per  $\text{m}^2$  and with swath widths from 21–168 m, corresponding to minimum and maximum footprints of 0.06 and 3.84 m. The laser pulse has a frequency of 7 Hz, and up to five returns are recorded per sounding. The maximum scan angle is  $20^\circ$ , reducing but not entirely eliminating the impact of relief displacement, shadowing, and

layover.

As a recent improvement over the profiling laser, namely, Rango et al. (2000) found the potential of moderate sampling density (1–2 m) scanning laser technology for providing accurate models of shrub-coppice-dune morphology to be viable, with excellent matches between a DEM from simple three-point interpolation and transit data from engineering surveys.

A twin-engine research aircraft has been used to collect airborne spectral (Exotech), thermal, three-band multispectral video, digital imagery, laser altimeter, and bidirectional reflectance data. Airborne campaigns have been scheduled to make measurements centered on the date of an overpass of Landsat or EOS-Terra. GPS navigation (Trimble Transpack II) was integrated with the systems on the airplane to measure the flight direction (bearing), altitude, time, ground speed, latitude, and longitude coordinates. Video imagery was obtained with a three-camera, multispectral, digital video imaging system (Everitt et al. 1995). The three cameras are visible near infrared (0.4–1.1  $\mu\text{m}$ ) equipped with yellow-green (0.555–0.565  $\mu\text{m}$ ), red (0.623–0.635  $\mu\text{m}$ ), and NIR (0.845–0.857  $\mu\text{m}$ ) filters. Imagery was acquired at altitudes between 300 and 3,000 m AGL, between 1000 and 1400 local time, under clear conditions during each campaign.

Since 2000, digital images have also been captured with a high-speed, multiband, digital capture camera designed and built by DuncanTech. It consists of a single F mount with three CCD arrays filtered by filters centered on 0.550, 0.650, and 0.800  $\mu\text{m}$  with band widths of 0.070, 0.040, and 0.065  $\mu\text{m}$  (Schiebe et al. 2001).

Airborne measurements of surface temperature were made with an Everest thermal sensor having a 15° field of view. An Exotech four-band radiometer was used to make radiance



measurements corresponding to the first four bands of the Landsat Thematic Mapper. The IRT and Exotech were mounted looking nadir. A second Exotech was placed on the ground looking upward to measure irradiance. A color video camera, borehole-sighted with the IRT and Exotech, recorded color images of the flight line. Each video frame was annotated with GPS data. Airborne data from these instruments were collected for the three flight lines at the approximate time of the Landsat or ASTER overpass. Each flight line was approximately 10 km long. Flights were made at altitudes of approximately 125 m and 300 m AGL with passes in opposite directions at each altitude on each flight line.

The aircraft flew an inexpensive hyperspectral imaging system (Yang et al. 2001) during fall 2002. The effective spectral range of this system is 0.467–0.932  $\mu\text{m}$  in 32–1,024 bands. This low-altitude hyperspectral capability should provide some valuable data for comparison with high-altitude, AVIRIS hyperspectral data.

### **High-Altitude Aircraft Data**

An improved camera for producing vertical aerial photographs with minimal distortion was developed by Sherman Fairchild in 1917 for the U.S. military (Thompson and Gruner 1980). By the early 1930s, the USDA started to systematically photograph agricultural lands in all states. Black-and-white aerial photographic coverage over parts of the Jornada Basin began in 1935. Aerial coverage has continued to the present in association with nationwide mapping projects or various remote-sensing research projects where color infrared photography is flown for comparison with new types of remote-sensing instrumentation.

To cover areas of the Jornada Basin other than the grids and transects, data have been acquired by aircraft since 1997. The flight lines were chosen to cover mesquite, transition, grass,

creosote, tarbush, and playa test sites as shown in figure 15-1. In 1997 the airplane flew both the Thematic Mapper Simulator (TMS) and the Thermal Infrared Multispectral Scanner (TIMS) instruments. TMS measures radiances in 12 bands ranging from the visible to thermal infrared; 7 bands are identical to the 7 bands of the Landsat TM. TIMS has six channels in the TIR, 8–12- $\mu\text{m}$  region of the electromagnetic spectrum.

The MASTER VIS, NIR, and TIR data were corrected for atmospheric effects using the MODTRAN path radiance model with atmospheric profiles appropriate for the conditions. All the profiles were adjusted for the surface temperature and humidity conditions observed by the weather station at the Jornada.

Even higher altitude aircraft coverage is periodically provided by the NASA ER-2 aircraft at an altitude of 20 km flying both the Airborne Visible/Infrared Imaging Spectrometer (AVIRIS) and the RC-10 mapping camera. The AVIRIS instrument has 224 detectors covering the entire spectral range from 0.380 to 2.500  $\mu\text{m}$ . These hyperspectral data are useful for vegetation mapping and can be compared with the ground-based ASD measurements. The RC-10 camera can also provide color infrared photography over the same area imaged by AVIRIS at 3–8-m resolution to compare with the multispectral 210-m resolution AVIRIS data.

### **Satellite Remote Sensing**

Landsat was the pioneering Earth resources technology satellite, and it is a very reliable platform. At present, Landsat 7 with the Enhanced TM + is operable. It provides coverage in six visible, near infrared, and mid-infrared channels with 30-m resolution; one thermal channel with 60-m resolution; and one panchromatic band with 15-m resolution. Because Landsat has been in existence since 1972 (in various instrument and wavelength configurations), it is treated as a

standard against which other sensor products are compared.

With a ground-projected field of view between NOAA-AVHRR and Landsat TM, the Moderate-Resolution Imaging Spectrometer (MODIS) instrument on the Terra satellite (and now the Aqua satellite also) is now providing coverage of earth every one to two days, acquiring data in 36 spectral bands. Two visible/near infrared bands nominally acquire data at 250-m resolution at nadir, 5 bands acquire data at 500-m resolution, and 29 bands (including the thermal bands) possess a 1-km resolution capability. The MODIS data are freely available through a number of Web sites, but some important data corrections are necessary for analysis.

The Advanced Spaceborne Thermal Emission and Reflection (ASTER) radiometer (Yamaguchi et al. 1998) also flies on Terra and has three subsystems to collect data: the visible and near infrared (four bands, 15-m resolution), the shortwave infrared (six bands, 30-m resolution), and the TIR (five bands, 60-m resolution). A stereo capability is available from ASTER in the visible and near infrared. The thermal coverage, however, is the most interesting because of its multiple bands and high resolution which allows estimation of surface emissivity.

The Ikonos satellite system (named from the Greek word for *image*), which was launched in 1999, operates in a multispectral mode (visible and near infrared bands) with a resolution of 4 m and in a panchromatic mode with a resolution of 1 m. The swath width of data acquisition is limited to 11 km. It has great flexibility by being able to point off-nadir to acquire data.

More recently, QuickBird was launched in 2001. It is similar to Ikonos but has an improved multispectral spatial resolution of 2.44 m and a panchromatic resolution of 0.61 m. It has a swath width of 16.5 km and an off-nadir pointing capability. It is usually possible to get

synchronous coverage over the Jornada test sites on the same day. NOAA-AVHRR, MODIS, and Landsat overpasses follow in quick succession, and ASTER can be scheduled to acquire data because Terra is already overhead at the same time. Although their revisit times are variable, data from Ikonos and QuickBird are possible at the same time (plus or minus a day) using their pointing capability.

### **Multiangular Reflectance Measurements and Thermal Infrared Analysis**

The bidirectional reflectance distribution function describes the angular distribution of scattered light from a surface with respect to that of solar irradiance on the surface. Thus, it is a potential source of both noise and information on the surface. It is accessed by sampling the bidirectional reflectance using sensors that view off-nadir and/or at varying sun zenith angles, these data often being called “multiangle,” “multiple-view angle,” or “multiangular.”

One of the objectives for the multispectral, thermal, infrared data from ASTER is to obtain both the surface temperature and multispectral emissivity from the five bands. The approach was demonstrated using aircraft data (Schmugge et al. 2001). The emissivity results using ASTER data from four Jornada sites for dates from May 9, 2000, to May 31, 2002, are given in figure 15-4.

There is good agreement amongst the ASTER results for all five channels for both the mesquite and transition sites. At the mesquite site, we made field measurements with the CIMEL 312 (Legrand et al. 2000) radiometer and found there was good agreement between the ground measurements for the dominant dark soil and the ASTER results. As seen in figure 15-4, there was reasonable consistency among the ASTER results for the five different days.

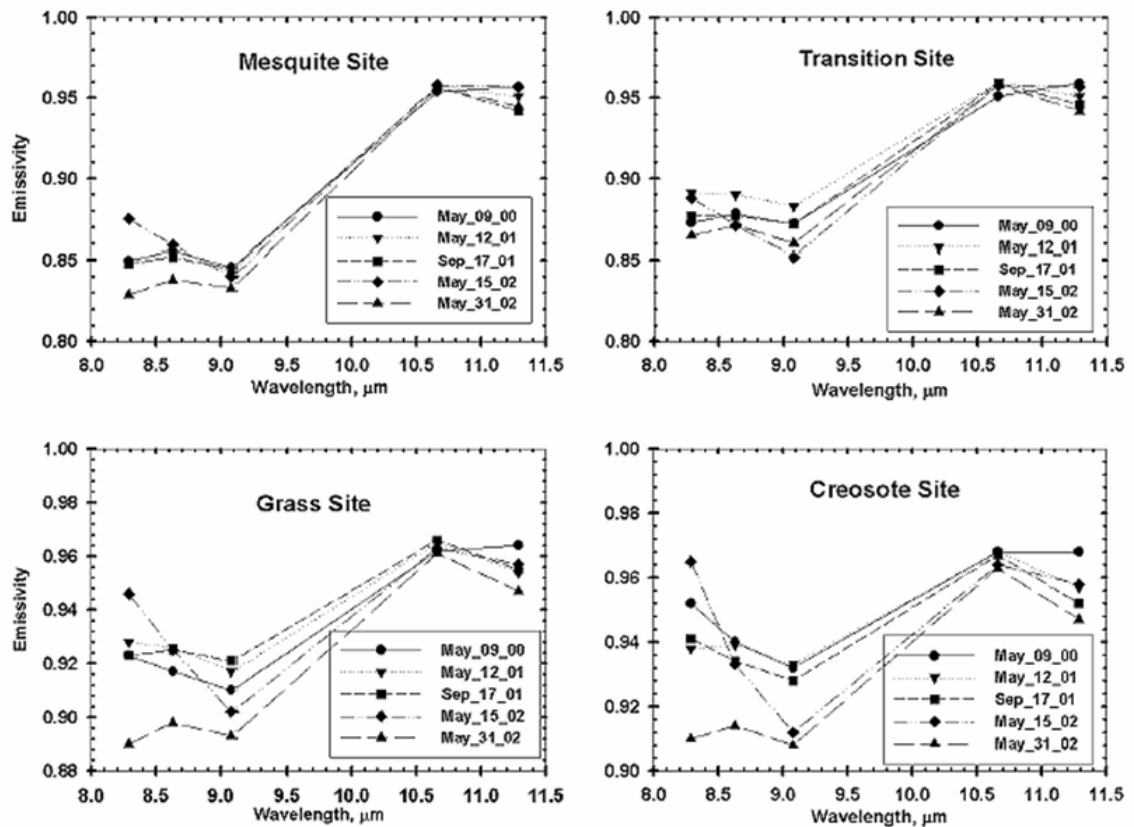


Fig. 15-4. ASTER emissivity results for four sites at the Jornada Experimental Range from five observation dates between 5/9/00 and 5/31/02.

The results from the grass and creosotebush sites show reasonably good agreement for the three dates in 2000 and 2001. However, the two dates in 2002 show consistently lower emissivity values, especially for the short wavelength (8–9  $\mu\text{m}$ ) channels. We suspect that this difference could be due to lower vegetation cover resulting from the drier than normal conditions during 2002.

Ground measurements of surface brightness temperature,  $T_B$ , are summarized in figure 15-5 for the four dates on which we have nearly coincident ground measurements and an ASTER overpass.

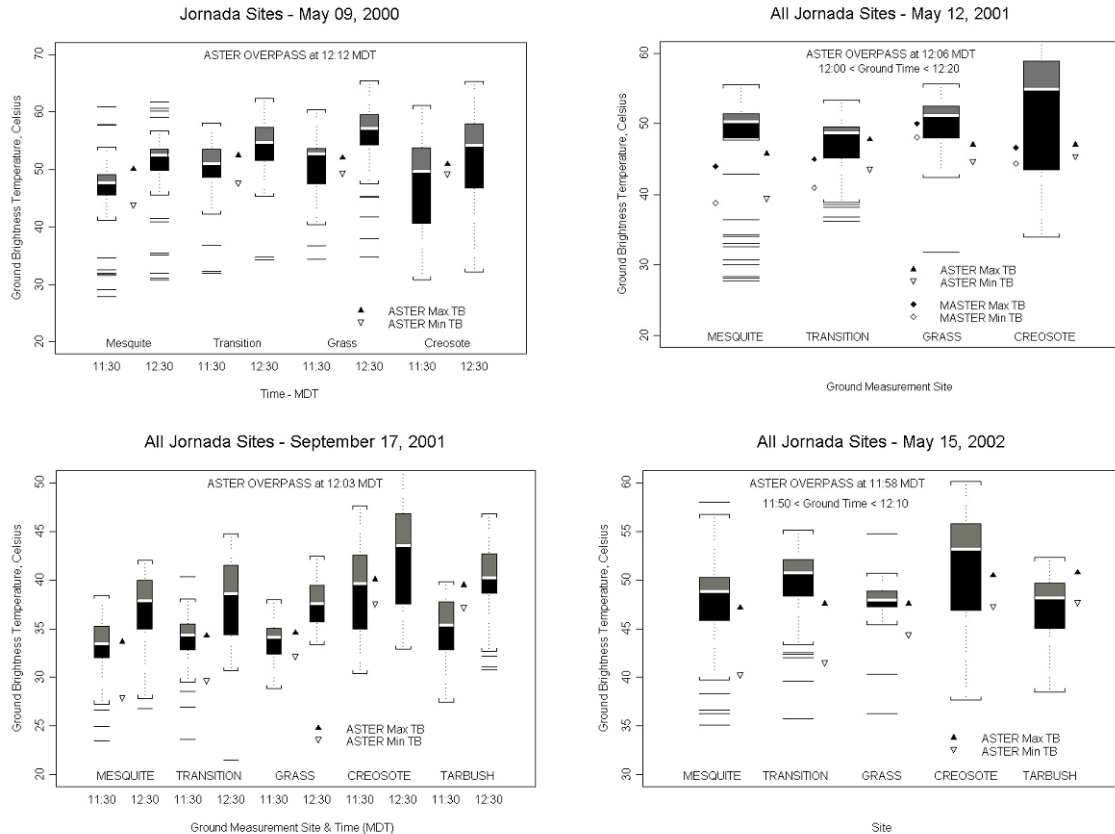


Fig. 15-5. ASTER brightness temperatures at the surface compared with nearly coincident ground observations. Note that the 5/12/01 case shows nearly coincident MASTER brightness temperatures.

The ground data are presented in box plots at the times bracketing the overpass (i.e., 1130 and 1230 MDT) or coincident with the overpass (about 1200 MDT) for the four sites. The box shows the range for 50% of the observations, and the bright line in the box indicates the median for the data. The lines represent outliers in the measurements beyond that expected for a normal distribution (indicated by the brackets). The range of  $T_B$  for the five ASTER channels is presented by the up-and-down triangles. It was expected that the broadband emissivity for the ground measurements would be within the range of those for the five ASTER channels and, thus,

the average ground  $T_B$  would be within the ASTER  $T_B$  range. It can be seen that there is reasonable agreement, but the ASTER data are a bit cooler. For the May 12, 2001, case, data from the aircraft instrument, MASTER, were also acquired. The range of MASTER  $T_{BS}$  is indicated by the triangles to the left of the box. The channels represented by this range cover approximately the same wavelength range as that covered by the ASTER channels. The agreement of MASTER and ASTER is quite good.

These results indicate that a temperature emissivity separation algorithm developed for use of ASTER data appears to work as well with the data from space as it did with the aircraft data presented earlier (Schmugge et al. 2001). This is encouraging for the application of the technique for mapping emissivity over large areas.

### **Large Area Coverage**

Two important capabilities are desirable for rangeland research in the Jornada Basin. The first is high-resolution, remote-sensing coverage over the entire basin or over large parts of the basin. Aircraft aerial photography is, of course, a possibility. Unfortunately, to acquire high-resolution data ( $< 1$  m), the airplane needs to fly at low to moderate altitude. As a result, many frames of aerial photography would be required to cover both CDRRC and JER and even more to cover the entire Jornada Basin. It is probably more efficient to use 0.61-m, panchromatic (or 2.44-m multispectral) resolution of the commercial QuickBird satellite to get the high-resolution coverage desired. It takes at least three swaths of the QuickBird multispectral sensor to get complete coverage of the Jornada Basin. The excellent resolution, however, may outweigh any difficulties in working with several different swaths, especially when rangelands are being assessed. Because this is a commercial satellite product that would require numerous swaths to

cover the entire Jornada Basin, the total cost of the image acquisition may become too expensive. With the drawbacks of getting both aerial photography or QuickBird data when needed and at a reasonable price, alternatives like the use of Unmanned Aerial Vehicles (UAVs) are currently being explored. Acquisition of high resolution images by UAVs has certain advantages over piloted aircraft missions including lower cost, increased safety, flexibility in mission planning, and closer proximity to target areas. UAV images at Jornada have been used to produce measurements used in rangeland health determinations like vegetated and bare soil cover percentages and gap and patch sizes at 5 cm resolution. Eventually, resource management agencies, rangeland consultants, and private land managers should be able to use small and lightweight UAVs to acquire improved data at a reasonable cost that can be used to enhance management decisions.

To get a landscape perspective at reasonable cost without mosaicing, Landsat TM data seem to be ideal. The entire Jornada Basin is covered in one frame. The 30-m, multispectral resolution is sufficient to see major dirt roads, stock tanks, a variety of rangeland treatments, playa lake basins, ecotones, and the aforementioned southwest to northeast depositional patterns. On later Landsat platforms, the ETM+ sensor additionally provides 15-m panchromatic data. Repetitive coverage is possible every 16 days and is usually acquired successfully because of frequent clear skies outside the heart of the monsoon rainy season. When very high-resolution imagery is not the primary goal, Landsat TM data are a very useful product for rangelands. The current Landsat platforms are old and becoming unreliable, so it is critical that follow-on Landsats be designed and launched very soon.

## **Conclusions**



Using a multifaceted remote-sensing approach allows a number of applications in rangeland situations. First, it permits extrapolation of point-and-plot knowledge to large areas of rangeland that would never be observed normally because of inaccessibility, cost, lack of manpower and a variety of other problems. Second, it could be used as part of a system of related measurements to monitor rangeland resources across vast areas. When the cost can be afforded, the presently available 0.61–2.44-m (or similar) resolution, multispectral data are so useful that they can take the place of aircraft photography. With growing competition, the cost of this high-resolution satellite data is expected to decline. We also see a real immediate opportunity for incorporating UAV acquired high resolution imagery into this mix of data and their applications. Our approach for remotely sensed data has provided a framework for testing new, experimental technologies and techniques, such as scanning LIDAR and multiangle remote sensing from air and space. The fusion of different types of remote sensing data, such as multispectral, hyperspectral, radar, laser, and thermal spectral regions, is also expected to greatly increase information content in the future.